

See discussions, stats, and author profiles for this publication at: <https://www.researchgate.net/publication/259392475>

The Effect of Amino Group Charge on the Photooxidation Kinetics of Aromatic Amino Acids.

ARTICLE in THE JOURNAL OF PHYSICAL CHEMISTRY A · DECEMBER 2013

Impact Factor: 2.69 · DOI: 10.1021/jp4097919 · Source: PubMed

CITATIONS

3

READS

25

4 AUTHORS, INCLUDING:



Natalya Saprygina

International Tomographic Center

7 PUBLICATIONS 14 CITATIONS

SEE PROFILE



Guenter Grampp

Graz University of Technology

156 PUBLICATIONS 1,347 CITATIONS

SEE PROFILE



Alexandra V Yurkovskaya

International Tomographic Center

123 PUBLICATIONS 1,389 CITATIONS

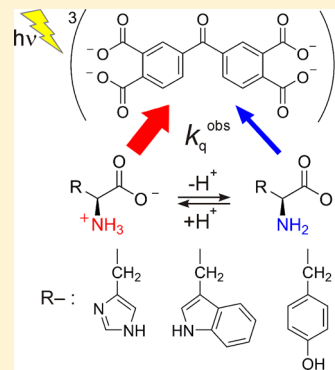
SEE PROFILE

Effect of Amino Group Charge on the Photooxidation Kinetics of Aromatic Amino Acids

Natalya N. Saprygina,^{†,‡} Olga B. Morozova,^{†,‡} Günter Grampp,[§] and Alexandra V. Yurkovskaya*,^{†,‡}[†]International Tomography Center, Institutskaya 3a, 630090 Novosibirsk, Russia[‡]Novosibirsk State University, Pirogova 2, 630090 Novosibirsk, Russia[§]Institute of Physical and Theoretical Chemistry, Graz University of Technology, Stremayrgasse 9, 8010 Graz, Austria

Supporting Information

ABSTRACT: The kinetics of the photooxidation of aromatic amino acids histidine (His), tyrosine (Tyr), and tryptophan (Trp) by 3,3',4,4'-benzophenonetetracarboxylic acid (TCBP) has been investigated in aqueous solutions using time-resolved laser flash photolysis and time-resolved chemically induced dynamic nuclear polarization. The pH dependence of quenching rate constants is measured within a large pH range. The chemical reactivities of free His, Trp, and Tyr and of their acetylated derivatives, *N*-AcHis, *N*-AcTyr, and *N*-AcTrp, toward TCBP triplets are compared to reveal the influence of amino group charge on the oxidation of aromatic amino acids. The bimolecular rate constants of quenching reactions between the triplet-excited TCBP in the fully deprotonated state and tryptophan, histidine, and tyrosine with a positively charged amino group are $k_q = 2.2 \times 10^9 \text{ M}^{-1} \text{ s}^{-1}$ ($4.9 < \text{pH} < 9.4$), $k_q = 1.6 \times 10^9 \text{ M}^{-1} \text{ s}^{-1}$ ($6.0 < \text{pH} < 9.2$), and $k_q = 1.5 \times 10^9 \text{ M}^{-1} \text{ s}^{-1}$ ($4.9 < \text{pH} < 9.0$), respectively. Tryptophan, histidine, and tyrosine with a neutral amino group quench the TCBP triplets with the corresponding rate constants $k_q = 8.0 \times 10^8 \text{ M}^{-1} \text{ s}^{-1}$ ($\text{pH} > 9.4$), $k_q = 3.0 \times 10^8 \text{ M}^{-1} \text{ s}^{-1}$ ($\text{pH} > 9.2$), and $k_q = (4.0\text{--}10.0) \times 10^8 \text{ M}^{-1} \text{ s}^{-1}$ ($9.0 < \text{pH} < 10.1$) that are close to those for the *N*-acetylated derivatives. Thus, it has been established that the presence of charged amino group changes oxidation rates by a significant factor; i.e., His with a positively charged amino group quenches the TCBP triplets 5 times more effectively than *N*-AcHis and His with a neutral amino group. The efficiency of quenching reaction between the TCBP triplets and Tyr and Trp with a positively charged amino group is about 3 times as high as that of both Tyr and Trp with a neutral amino group, *N*-AcTyr and *N*-AcTrp.



INTRODUCTION

There is considerable interest in a long-range electron transfer in biosystems that has drawn much experimental evidence for a number of peptides and proteins.^{1–6} Most of the observations refer to tryptophan and tyrosine residues, for which electron transfer was detected by means of transient optical spectroscopy^{7–9} and time-resolved chemically induced dynamic nuclear polarization (TR-CIDNP).^{10,11} The latter is especially useful when it is difficult or even impossible to initiate radical reactions under conditions needed for optical detection. CIDNP is also used to study the reactions of optically silent radicals, such as the histidyl ones.¹² However, the study of ET reactions, involving a histidyl radical, faces difficulties because among aromatic amino acids, histidine is usually poorly competitive for the triplet-excited photosensitizers such as flavin and dipyrindyl derivatives.^{13–17} Thus, to study radical reactions, involving the radicals of all aromatic amino acids, one should search for a dye whose triplet excited state could be quenched by tryptophan, tyrosine, and histidine with comparable efficiencies, which results in the formation of radical pairs, spin evolution of which gives rise to detectable CIDNP effects. In ref 18 it was reported that the aromatic amino acids Trp, His, and Tyr quench benzophenone triplets with comparable rate constants in a water–acetonitrile mixture

at pH 7. Thus, the use of the triplet-excited benzophenone derivatives could be suitable for our purpose.

In this paper, we report on the quenching of the triplet-excited 3,3',4,4'-benzophenonetetracarboxylic acid, ³TCBP, by aromatic amino acids and their *N*-acetyl derivatives in aqueous solution within a wide pH range studied by laser flash photolysis. The transient optical detection of the excited dye triplets is supplemented by measurements of CIDNP effects arising during the spin evolution of radical pairs formed as a result of triplet quenching. The TR-CIDNP technique makes it possible to detect the so-called geminate CIDNP arising in the nanosecond time scale in the products of the geminate recombination of spin-correlated radical pairs. The amplitude and the phase of geminate CIDNP signals encode the mechanism of the formation of a radical pair and its magneto-resonance parameters. The radical reaction products are recorded in the NMR spectrum, which allows us to resolve the signals of individual nuclei in a molecule.

Received: October 2, 2013

Revised: December 17, 2013

Published: December 19, 2013

■ EXPERIMENTAL SECTION

Laser Flash Photolysis. The samples sealed in a rectangular cell (1 × 1 cm) were irradiated with a Lambda Physik LPX-120 XeCl excimer laser (308 nm, pulse energy up to 100 mJ, 10 ns). The monitoring system consisted of a xenon lamp 150 W, a Hamamatsu R928 photomultiplier tube, a OBB/PTI monochromator model 101/102, and a digital storage oscilloscope 9410A LeCroy.

The concentration of TCBP in solutions in all LFP measurements was 1×10^{-4} M so as to avoid the triplet–triplet annihilation. All solutions were prepared in buffered aqueous solutions at room temperature. Prior to irradiation the samples were bubbled with argon for 15 min to remove dissolved oxygen. The buffer solutions with a concentration of 0.01 M were prepared in double distilled H₂O with (a) HCl–KH₂PO₄, pH = 3.0–5.0, (b) KH₂PO₄–Na₂HPO₄, pH = 5.0–9.0, and (c) Na₂HPO₄–NaOH, pH = 9.0–11.0. The values pH < 3 and pH > 11 were adjusted with HCl and NaOH, respectively.

Time-Resolved CIDNP. Our TR-CIDNP setup has been described in detail elsewhere.¹⁹ The samples were bubbled with argon for 15 min prior to irradiation and sealed in a standard NMR Pyrex ampule. The irradiation of the samples was performed in the probe of a 200 MHz Bruker DPX-200 NMR spectrometer (magnetic field is 4.7 T, resonance frequency of protons is 200 MHz) by the pulses of a COMPEX Lambda Physik XeCl excimer laser (wavelength 308 nm, output pulse energy up to 150 mJ). Light to the sample was guided through the optical system including a spherical lens, prism, and light-guide glass fiber (diameter 5 mm). The TR-CIDNP spectra were obtained using the following protocol: first, the reactant nuclear spin states were saturated using a pulsed broad-band homonuclear decoupler; thereafter, the spectrometer triggered the laser, and then the detecting radio frequency (RF) pulse of 1 μs duration was applied. The laser pulse was synchronized with the front edge of the pulse.

All ¹H NMR measurements were performed in D₂O. The acidity of NMR samples was varied using small amounts of DCl or NaOD. As the pH in D₂O solutions was measured with an H₂O calibrated pH-meter, the pH readings in this case corresponded to the so-called pH* values. Therefore, the NMR and TR-CIDNP data were evaluated using the pK_a* values instead of the normal pK_a according to $pK_a = 0.929pK_a^* + 0.42$.²⁰

The concentration of TCBP in CIDNP experiments was 2×10^{-3} M to avoid sample depletion upon laser irradiation. The concentrations of over reactants were 4.0×10^{-2} M (His, N-AcHis, His-His, His-Phe, Phe-His), 2.2×10^{-3} M (Tyr, N-AcTyr), and 1.1×10^{-3} M (Trp, N-AcTrp).

Chemicals. Compounds with the corresponding structures and abbreviations are listed in Table 1. L-Histidine, N-acetyl-L-histidine, L-tyrosine, N-acetyl-L-tyrosine, L-tryptophan, N-acetyl-L-tryptophan, 3,3',4,4'-benzophenonetetracarboxylic acid, DCl, NaOD (30% solution in D₂O), and D₂O were used as received from Sigma-Aldrich. L-Histidine-L-histidine and L-histidine-L-phenylalanine were purchased from Bachem and used without further purification. L-Phenylalanine-L-histidine was synthesized using activated ester BOC strategies by standard methods.

■ RESULTS

The protonation forms of all relevant reactants are summarized in Table 2. The acidity constants used to calculate the equilibrium concentrations of acids and their conjugated bases in LFP data simulations and the pK_a* values applied for TR-CIDNP data evaluation are listed in Table 1. TCBP can exist in one of the five protonation states. The corresponding acidity constants K_{a1}–K_{a4} were unavailable in the literature. Earlier, the two ground states pK_{a1} = 3.2 and pK_{a2} = 5.2 estimated using UV–vis spectroscopy and the two triplet excited states pK_{a1} = 2.1 and pK_{a2} = 4.7 obtained by triplet–triplet absorbance titration have been published.²⁵ Using the dependences of ¹H and ¹³C chemical shifts on pH, we have determined the acidity constants of TCBP in D₂O: pK_{a1}* = 2.5 ± 0.1 , pK_{a2}* = 2.7 ± 0.1 , pK_{a3}* = 4.5 ± 0.1 , and pK_{a4}* = 5.2 ± 0.1 . Simulating the chemical shift dependences with four pK_a values has led to better agreement than that using two pK_a values. However, the accuracy of our LFP and CIDNP experiments was lower than the accuracy of chemical shifts titration experiments. Therefore, in our simulations of the LFP and CIDNP data, we have considered TCBP a dibasic acid with two mean acidity constants pK_{a1}* = 2.7, pK_{a2}* = 4.8 in D₂O and pK_{a1} = 2.9, pK_{a2} = 4.9 in H₂O. Using the molar dye fractions calculated from the acidity constants of the TCBP ground state we have obtained good quality fits, probably, due to the fact that the difference in pK_a values between the triplet and the ground states of TCBP is insufficient within our experimental accuracy. The protonation state of the carboxylic group of both amino acids (pK_a ~ 2) and N-acetylated amino acids (pK_a ~ 3.5) is not explicitly shown in Table 2. Within the experimental accuracy of our LFP and CIDNP measurements, the acidity constant of the carboxylic group could be conventionally considered at 2.9, so as pK_{a1} of TCBP. Table 2 contains reactants' net charges that include the charge of the carboxylic group of amino acids as well.

Laser Flash Photolysis. The triplet–triplet annihilation was minor because of the low TCBP concentration (1×10^{-4} M). The decay of the triplet TCBP was measured at both 590 nm (pH < pK_{a2}^{TCBP} = 4.9) and 550 nm (pH > pK_{a2}^{TCBP} = 4.9),²⁵ where the triplet-excited dye has the maxima of absorption. Irradiation of TCBP solutions without a quencher results in the triplet-excited TCBP, which decays mainly by the first-order kinetics with $k_d = (5.5\text{--}8) \times 10^5 \text{ s}^{-1}$.^{25,26} In the presence of the quencher, the triplet TCBP interacts with it by the pseudo-first-order kinetics. As a result, from the triplet decay of TCBP at fixed wavelengths, the observed quenching rate constant, k_q^{obs} , was obtained using the Stern–Volmer relation (eq 1a or eq 1b):

$$k_{\text{obs}} = k_d + k_q^{\text{obs}}[Q] \quad (1a)$$

$$\frac{{}^3\tau_0}{\tau} = 1 + {}^3\tau_0 k_q^{\text{obs}}[Q] \quad (1b)$$

where k_d is the rate constant of the triplet TCBP decay, k_q^{obs} is the observed quenching rate constant, ${}^3\tau_0 = (1/k_d)$ is the lifetime of the triplet TCBP in solutions without a quencher, $\tau = (1/k_{\text{obs}})$ is the actual lifetime of the triplet TCBP in the presence of a quencher, and $[Q]$ is the quencher concentration. In all the systems studied at 550 nm (or 590 nm), the time scale was chosen so that the total decay was a combination of two parallel reactions, i.e., the decay of the TCBP triplets and the first-order growth of both the TCBP radicals (TCBP•–

Table 1. List of Compounds

Compound	Abbreviation	Structure	pK_a	pK_a^*
3,3',4,4'-benzophenone tetracarboxylic acid	TCBP		2.9; 4.9 ^(a)	2.7; 4.8
L-histidine	His		1.8; 6.0; 9.2 ²¹ ; 14.3 ^(b)	1.5; 6.0; 9.5; 14.9
N-acetyl-L-histidine	N-AcHis		~3.5 ^(c) ; 7.0 ²² ; 14.3 ²²	~3.3; 7.1; 14.9
L-tyrosine	Tyr		2.2; 9.0; 10.1 ²¹	1.9; 9.2; 10.4
N-acetyl-L-tyrosine	N-AcTyr		~3.5 ^(b) ; 10.2 ^(a)	~3.3; 10.5
L-tryptophan	Trp		2.4; 9.4 ²¹	2.1; 9.7
N-acetyl-L-tryptophan	N-AcTrp		3.4 ²³	3.2
L-histidine-L-histidine	His-His		5.7; 6.7; 7.9 ^(a)	5.7; 6.8; 8.0
L-histidine-L-phenylalanine	His-Phe		6.1; 7.8 ^(a)	6.1; 7.9
L-phenylalanine-L-histidine	Phe-His		6.7; 7.8 ^(a)	6.8; 7.9

^aThe values of pK_a , unavailable in the literature, were determined experimentally from the dependences of chemical shifts on pH. See the Supporting Information for details. ^bThe value of pK_{a4} for His is unavailable in the literature; the corresponding pK_a value for N-AcHis is equal to 14.3.²² ^cThe typical pK_a value for the carboxylic group in peptides and N-acetylated derivatives of amino acids is ~3.5.^{23,24}

absorbs at $\lambda_{\max} = 630 \text{ nm}$)²⁵ and the radicals of amino acids (for TyrO^\bullet $\lambda_{\max} = 407 \text{ nm}$,²⁷ for $\text{Trp}^{+\bullet}$ $\lambda_{\max} = 510 \text{ nm}$,^{28,29} for Trp^\bullet $\lambda_{\max} = 580 \text{ nm}$ ^{28,29}). A subsequent, relatively slow decay of radicals was neglected at the time scale chosen. The transient absorbance (A) was simulated in terms of the following equation:

$$A = A_T + A_R \quad (2)$$

where A_T or A_R is the transient absorbance TCBP triplets or radicals.

$$A_T = A_0 \exp(-k_{\text{obs}}t) + A_{\text{er}} \quad (2a)$$

$$A_R = A^\infty(1 - \exp(-k_{\text{obs}}t)) \quad (2b)$$

where A_0 and A^∞ are the absorbance at time 0 and infinity, respectively. A_{er} takes account of the fact that due to the

Table 2. Quenching Rate Constants of TCBP Triplet by Quenchers (k_{qi}) and the Relative CIDNP Magnitudes for Different Quenchers $q_i \times p_i$

quencher	pH region	reactant pair	net charges of reactants (TCBP/amino acid)	k_{qi} ($M^{-1} s^{-1}$)	$q_i \times p_i^a$
histidine	pH < 2.9	TCBPH ₄ and NH ₃ ⁺ HisH ₂ ⁺	0/+2	<1.0 × 10 ⁶	0
	2.9 < pH < 4.9	TCBPH ₂ ²⁻ and NH ₃ ⁺ HisH ₂ ⁺	-2/+1	4.3 × 10 ⁸	0.14
	4.9 < pH < 6.0	TCBP ⁴⁻ and NH ₃ ⁺ HisH ₂ ⁺	-4/+1	1.0 × 10 ⁸	0.49
	6.0 < pH < 9.2	TCBP ⁴⁻ and NH ₃ ⁺ HisH	-4/0	1.6 × 10 ⁹	1
	9.2 < pH < 14.3	TCBP ⁴⁻ and NH ₂ HisH	-4/-1	3.0 × 10 ⁸	0.47
N-acetylhistidine	pH > 14.3	TCBP ⁴⁻ and NH ₂ His ⁻	-4/-2	n/a ^b	0
	pH < 2.9	TCBPH ₄ and N-AcHisH ₂ ⁺	0/+1	<1.0 × 10 ⁶	0
	2.9 < pH < 4.9	TCBPH ₂ ²⁻ and N-AcHisH ₂ ⁺	-2/0	7.7 × 10 ⁷	0.12
	4.9 < pH < 7.0	TCBP ⁴⁻ and N-AcHisH ₂ ⁺	-4/0	1.9 × 10 ⁷	0.06
	7.0 < pH < 14.3	TCBP ⁴⁻ and N-AcHisH	-4/-1	3.1 × 10 ⁸	0.41
tyrosine	pH > 14.3	TCBP ⁴⁻ and N-AcHis ⁻	-4/-2	n/a ^b	0
	pH < 2.9	TCBPH ₄ and NH ₃ ⁺ TyrOH	0/+1	2.1 × 10 ⁹	0.9
	2.9 < pH < 4.9	TCBPH ₂ ²⁻ and NH ₃ ⁺ TyrOH	-2/0	1.9 × 10 ⁹	0.97
	4.9 < pH < 9.0	TCBP ⁴⁻ and NH ₃ ⁺ TyrOH	-4/0	1.5 × 10 ⁹	1
	9.0 < pH < 10.1	TCBP ⁴⁻ and NH ₂ TyrOH	-4/-1	(4.0–10.0) × 10 ^{8c}	0.66
N-acetyltyrosine	pH > 10.1	TCBP ⁴⁻ and NH ₂ TyrO ⁻	-4/-2	<1.0 × 10 ⁶	0
	pH < 2.9	TCBPH ₄ and N-AcTyrOH	0/0	2.7 × 10 ⁹	1
	2.9 < pH < 4.9	TCBPH ₂ ²⁻ and N-AcTyrOH	-2/-1	1.7 × 10 ⁹	0.7
	4.9 < pH < 10.1	TCBP ⁴⁻ and N-AcTyrOH	-4/-1	4.2 × 10 ⁸	0.18
	pH > 10.1	TCBP ⁴⁻ and N-AcTyrO ⁻	-4/-2	<1.0 × 10 ⁶	0
tryptophan	pH < 2.9	TCBPH ₄ and NH ₃ ⁺ Trp	0/+1	3.5 × 10 ⁹	0.22 ^{d/0.89}
	2.9 < pH < 4.9	TCBPH ₂ ²⁻ and NH ₃ ⁺ Trp	-2/0	3.5 × 10 ⁹	1.05
	4.9 < pH < 9.4	TCBP ⁴⁻ and NH ₃ ⁺ Trp	-4/0	2.2 × 10 ⁹	0.99
	pH > 9.4	TCBP ⁴⁻ and NH ₂ Trp	-4/-1	8.0 × 10 ⁸	0.39
N-acetyltryptophan	pH < 2.9	TCBPH ₄ and N-AcTrp	0/0	3.4 × 10 ⁹	0.55 ^{d/0.75}
	2.9 < pH < 4.9	TCBPH ₂ ²⁻ and N-AcTrp	-2/-1	2.1 × 10 ⁹	0.34
	pH > 4.9	TCBP ⁴⁻ and N-AcTrp	-4/-1	7.8 × 10 ⁸	0.3

^a $q_i \times p_i$ parameters were calculated using pK_a^* values for D₂O solutions. ^b k_{qi} value was not determined because the ionic strength of the solution was not constant upon increasing of pH from 12 to 14. ^c It was impossible to determine this value with high accuracy due to a minor difference between pK_{a2} and pK_{a3} of Tyr. ^d Degenerate electron exchange reaction at pH values below $pK_a = 4.3^{29,31}$ of tryptophanyl radical cation: ${}^P\text{TrpH}^{+\bullet} + \text{TrpH} \xrightarrow{k_{ex}} {}^b\text{TrpH} + \text{TrpH}^{+\bullet}$ (polarization is denoted as "P") effect on CIDNP magnitude. Therefore, $pK_a = 4.3$ was considered in the geminate CIDNP intensity simulation.

instrumental error, at infinity A_T is not zero but some small value.

The values of k_q^{obs} were calculated using eq 1b with k_{obs} obtained from eq 2 at each quencher concentration.

The observed pH dependences of the quenching rate constant k_q^{obs} were characterized by the method from ref 30. The pH dependences of the quenching rate constants were split into several pH regions with the bounds at the pK_a values of initial reactants. In the pH region chosen, each pair of reactants (triplet TCBP and a quencher) reacts with the so-called intrinsic quenching rate constant (k_{qi}). To figure out the observed k_q^{obs} , it is necessary to sum up k_{qi} , multiplied by the molar fractions of the corresponding species in terms of eq 3.

$$k_q^{\text{obs}} = \sum_i k_{qi} \times \alpha(\text{dye}) \times \alpha(\text{quencher}) \quad (3)$$

Finally, the treatment of pH dependences using eq 3 by the least-squares fit with the known parameters (k_q^{obs} , K_{a1} , $[H^+]$) has provided the intrinsic k_{qi} values.

Quenching by Tryptophan and N-Acetyltryptophan.

At 308 nm and at the chosen concentrations, the absorbance of Trp and N-AcTrp is much smaller than that of TCBP. Thus, irradiating the TCBP and Trp (or N-AcTrp) solution results first in the triplet-excited TCBP and then in the quenching reaction. The pH dependences of k_q^{obs} shown in Figure 1 (see Tables 1 and 2 for parameters) were described by eqs 4a (for

Trp) and 4b (for N-AcTrp). Table 2 contains the main reactant pairs for each pH region and the corresponding quenching rate constants, k_{qi} , obtained by the best fit (solid line, Figure 1).

$$\begin{aligned}
 k_q^{\text{obs}} = & k_{q1} \times \frac{[H^+]^2}{[H^+]^2 + K_{a1}^{\text{TCBP}}[H^+]^2 + K_{a1}^{\text{TCBP}}K_{a2}^{\text{TCBP}}} \\
 & \times \frac{[H^+]}{[H^+] + K_{a1}^{\text{Trp}}} \\
 & + k_{q2} \times \frac{K_{a1}^{\text{TCBP}}[H^+]^2}{[H^+]^2 + K_{a1}^{\text{TCBP}}[H^+]^2 + K_{a1}^{\text{TCBP}}K_{a2}^{\text{TCBP}}} \\
 & \times \frac{[H^+]}{[H^+] + K_{a1}^{\text{Trp}}} \\
 & + k_{q3} \times \frac{K_{a1}^{\text{TCBP}}K_{a2}^{\text{TCBP}}}{[H^+]^2 + K_{a1}^{\text{TCBP}}[H^+]^2 + K_{a1}^{\text{TCBP}}K_{a2}^{\text{TCBP}}} \\
 & \times \frac{[H^+]}{[H^+] + K_{a1}^{\text{Trp}}} \\
 & + k_{q4} \times \frac{K_{a1}^{\text{TCBP}}K_{a2}^{\text{TCBP}}}{[H^+]^2 + K_{a1}^{\text{TCBP}}[H^+]^2 + K_{a1}^{\text{TCBP}}K_{a2}^{\text{TCBP}}} \\
 & \times \frac{K_{a1}^{\text{Trp}}}{[H^+] + K_{a1}^{\text{Trp}}} \quad (4a)
 \end{aligned}$$

$$k_q^{\text{obs}} = k_{q1} \times \frac{[\text{H}^+]^2}{[\text{H}^+]^2 + K_{a1}^{\text{TCBP}}[\text{H}^+]^2 + K_{a1}^{\text{TCBP}}K_{a2}^{\text{TCBP}}} + k_{q2} \times \frac{K_{a1}^{\text{TCBP}}[\text{H}^+]^2}{[\text{H}^+]^2 + K_{a1}^{\text{TCBP}}[\text{H}^+]^2 + K_{a1}^{\text{TCBP}}K_{a2}^{\text{TCBP}}} + k_{q3} \times \frac{K_{a1}^{\text{TCBP}}K_{a2}^{\text{TCBP}}}{[\text{H}^+]^2 + K_{a1}^{\text{TCBP}}[\text{H}^+]^2 + K_{a1}^{\text{TCBP}}K_{a2}^{\text{TCBP}}} \quad (4b)$$

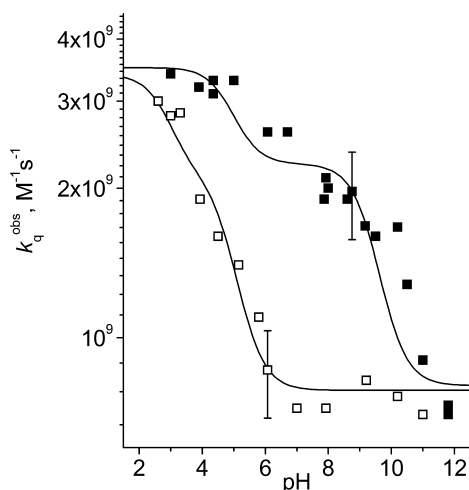


Figure 1. pH dependences of the observed quenching rate constant for the reaction of triplet TCBP with Trp (solid squares) and with *N*-AcTrp (open squares). Solid lines are the simulations from eqs 4a and 4b.

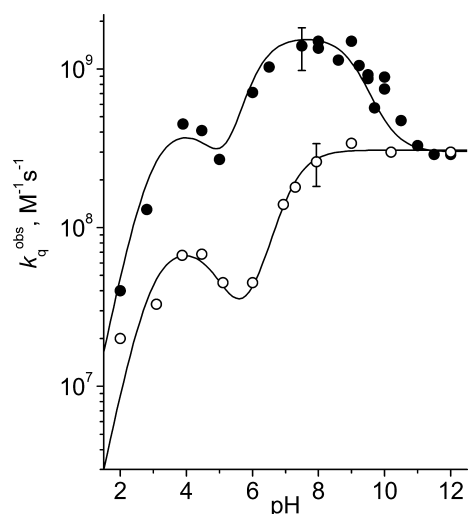


Figure 2. pH dependences of the observed quenching rate constant for the reaction of triplet TCBP with His (solid circles) and with *N*-AcHis (open circles). Solid lines are the simulations from eqs 5a and 5b.

Quenching by Histidine and *N*-Acetylhistidine. The relevant reactant pairs at different pH values are listed in Table 2. Because histidine does not absorb light in UV and visible regions, the irradiation of solution containing TCBP and His or *N*-AcHis gives the triplet-excited TCBP with transient absorption spectra close to the published ones.^{25,26} The pH dependences of k_q^{obs} obtained in the reaction of the triplet

TCBP with His and *N*-AcHis were treated according to eqs 5a and 5b (see Tables 1 and 2 for parameters). The values obtained from the best fit (solid line, Figure 2) are also summarized in Table 2.

$$k_q^{\text{obs}} = k_{q1} \times \frac{[\text{H}^+]^2}{[\text{H}^+]^2 + K_{a1}^{\text{TCBP}}[\text{H}^+]^2 + K_{a1}^{\text{TCBP}}K_{a2}^{\text{TCBP}}} \times \frac{[\text{H}^+]^2}{[\text{H}^+]^2 + K_{a1}^{\text{His}}[\text{H}^+] + K_{a1}^{\text{His}}K_{a2}^{\text{His}}} + k_{q2} \times \frac{K_{a1}^{\text{TCBP}}[\text{H}^+]^2}{[\text{H}^+]^2 + K_{a1}^{\text{TCBP}}[\text{H}^+]^2 + K_{a1}^{\text{TCBP}}K_{a2}^{\text{TCBP}}} \times \frac{[\text{H}^+]^2}{[\text{H}^+]^2 + K_{a1}^{\text{His}}[\text{H}^+] + K_{a1}^{\text{His}}K_{a2}^{\text{His}}} + k_{q3} \times \frac{K_{a1}^{\text{TCBP}}K_{a2}^{\text{TCBP}}}{[\text{H}^+]^2 + K_{a1}^{\text{TCBP}}[\text{H}^+]^2 + K_{a1}^{\text{TCBP}}K_{a2}^{\text{TCBP}}} \times \frac{[\text{H}^+]^2}{[\text{H}^+]^2 + K_{a1}^{\text{His}}[\text{H}^+] + K_{a1}^{\text{His}}K_{a2}^{\text{His}}} + k_{q4} \times \frac{K_{a1}^{\text{TCBP}}K_{a2}^{\text{TCBP}}}{[\text{H}^+]^2 + K_{a1}^{\text{TCBP}}[\text{H}^+]^2 + K_{a1}^{\text{TCBP}}K_{a2}^{\text{TCBP}}} \times \frac{K_{a1}^{\text{His}}[\text{H}^+]}{[\text{H}^+]^2 + K_{a1}^{\text{His}}[\text{H}^+] + K_{a1}^{\text{His}}K_{a2}^{\text{His}}} + k_{q5} \times \frac{K_{a1}^{\text{TCBP}}K_{a2}^{\text{TCBP}}}{[\text{H}^+]^2 + K_{a1}^{\text{TCBP}}[\text{H}^+]^2 + K_{a1}^{\text{TCBP}}K_{a2}^{\text{TCBP}}} \times \frac{K_{a1}^{\text{His}}K_{a2}^{\text{His}}}{[\text{H}^+]^2 + K_{a1}^{\text{His}}[\text{H}^+] + K_{a1}^{\text{His}}K_{a2}^{\text{His}}} \quad (5a)$$

$$k_q^{\text{obs}} = k_{q1} \times \frac{[\text{H}^+]^2}{[\text{H}^+]^2 + K_{a1}^{\text{TCBP}}[\text{H}^+]^2 + K_{a1}^{\text{TCBP}}K_{a2}^{\text{TCBP}}} \times \frac{[\text{H}^+]}{[\text{H}^+] + K_{a1}^{\text{N-AcHis}}} + k_{q2} \times \frac{K_{a1}^{\text{TCBP}}[\text{H}^+]^2}{[\text{H}^+]^2 + K_{a1}^{\text{TCBP}}[\text{H}^+]^2 + K_{a1}^{\text{TCBP}}K_{a2}^{\text{TCBP}}} \times \frac{[\text{H}^+]}{[\text{H}^+] + K_{a1}^{\text{N-AcHis}}} + k_{q3} \times \frac{K_{a1}^{\text{TCBP}}K_{a2}^{\text{TCBP}}}{[\text{H}^+]^2 + K_{a1}^{\text{TCBP}}[\text{H}^+]^2 + K_{a1}^{\text{TCBP}}K_{a2}^{\text{TCBP}}} \times \frac{[\text{H}^+]}{[\text{H}^+] + K_{a1}^{\text{N-AcHis}}} + k_{q4} \times \frac{K_{a1}^{\text{TCBP}}K_{a2}^{\text{TCBP}}}{[\text{H}^+]^2 + K_{a1}^{\text{TCBP}}[\text{H}^+]^2 + K_{a1}^{\text{TCBP}}K_{a2}^{\text{TCBP}}} \times \frac{K_{a1}^{\text{N-AcHis}}}{[\text{H}^+] + K_{a1}^{\text{N-AcHis}}} \quad (5b)$$

Quenching by Tyrosine and *N*-Acetyltyrosine. The dependences of the observed quenching rate constants on pH are presented in Figure 3. The pH dependences of k_q^{obs} obey eqs 6a and 6b (see Tables 1 and 2 for parameters). The k_q^{obs} values obtained from the best fit (solid line, Figure 3) are shown in Table 2.

$$\begin{aligned}
k_q^{\text{obs}} = & k_{q1} \times \frac{[\text{H}^+]^2}{[\text{H}^+]^2 + K_{a1}^{\text{TCBP}}[\text{H}^+]^2 + K_{a1}^{\text{TCBP}}K_{a2}^{\text{TCBP}}} \\
& \times \frac{[\text{H}^+]^2}{[\text{H}^+]^2 + K_{a1}^{\text{Tyr}}[\text{H}^+] + K_{a1}^{\text{Tyr}}K_{a2}^{\text{Tyr}}} \\
& + k_{q2} \times \frac{K_{a1}^{\text{TCBP}}[\text{H}^+]^2}{[\text{H}^+]^2 + K_{a1}^{\text{TCBP}}[\text{H}^+]^2 + K_{a1}^{\text{TCBP}}K_{a2}^{\text{TCBP}}} \\
& \times \frac{[\text{H}^+]^2}{[\text{H}^+]^2 + K_{a1}^{\text{Tyr}}[\text{H}^+] + K_{a1}^{\text{Tyr}}K_{a2}^{\text{Tyr}}} \\
& + k_{q3} \times \frac{K_{a1}^{\text{TCBP}}K_{a2}^{\text{TCBP}}}{[\text{H}^+]^2 + K_{a1}^{\text{TCBP}}[\text{H}^+]^2 + K_{a1}^{\text{TCBP}}K_{a2}^{\text{TCBP}}} \\
& \times \frac{[\text{H}^+]^2}{[\text{H}^+]^2 + K_{a1}^{\text{Tyr}}[\text{H}^+] + K_{a1}^{\text{Tyr}}K_{a2}^{\text{Tyr}}} \\
& + k_{q4} \times \frac{K_{a1}^{\text{TCBP}}K_{a2}^{\text{TCBP}}}{[\text{H}^+]^2 + K_{a1}^{\text{TCBP}}[\text{H}^+]^2 + K_{a1}^{\text{TCBP}}K_{a2}^{\text{TCBP}}} \\
& \times \frac{K_{a1}^{\text{Tyr}}[\text{H}^+]}{[\text{H}^+]^2 + K_{a1}^{\text{Tyr}}[\text{H}^+] + K_{a1}^{\text{Tyr}}K_{a2}^{\text{Tyr}}} \\
& + k_{q5} \times \frac{K_{a1}^{\text{TCBP}}K_{a2}^{\text{TCBP}}}{[\text{H}^+]^2 + K_{a1}^{\text{TCBP}}[\text{H}^+]^2 + K_{a1}^{\text{TCBP}}K_{a2}^{\text{TCBP}}} \\
& \times \frac{K_{a1}^{\text{Tyr}}K_{a2}^{\text{Tyr}}}{[\text{H}^+]^2 + K_{a1}^{\text{Tyr}}[\text{H}^+] + K_{a1}^{\text{Tyr}}K_{a2}^{\text{Tyr}}} \quad (6a)
\end{aligned}$$

$$\begin{aligned}
k_q^{\text{obs}} = & k_{q1} \times \frac{[\text{H}^+]^2}{[\text{H}^+]^2 + K_{a1}^{\text{TCBP}}[\text{H}^+]^2 + K_{a1}^{\text{TCBP}}K_{a2}^{\text{TCBP}}} \\
& \times \frac{[\text{H}^+]}{[\text{H}^+] + K_{a1}^{\text{N-AcTyr}}} \\
& + k_{q2} \times \frac{K_{a1}^{\text{TCBP}}[\text{H}^+]^2}{[\text{H}^+]^2 + K_{a1}^{\text{TCBP}}[\text{H}^+]^2 + K_{a1}^{\text{TCBP}}K_{a2}^{\text{TCBP}}} \\
& \times \frac{[\text{H}^+]}{[\text{H}^+] + K_{a1}^{\text{N-AcTyr}}} \\
& + k_{q3} \times \frac{K_{a1}^{\text{TCBP}}K_{a2}^{\text{TCBP}}}{[\text{H}^+]^2 + K_{a1}^{\text{TCBP}}[\text{H}^+]^2 + K_{a1}^{\text{TCBP}}K_{a2}^{\text{TCBP}}} \\
& \times \frac{[\text{H}^+]}{[\text{H}^+] + K_{a1}^{\text{N-AcTyr}}} \\
& + k_{q4} \times \frac{K_{a1}^{\text{TCBP}}K_{a2}^{\text{TCBP}}}{[\text{H}^+]^2 + K_{a1}^{\text{TCBP}}[\text{H}^+]^2 + K_{a1}^{\text{TCBP}}K_{a2}^{\text{TCBP}}} \\
& \times \frac{K_{a1}^{\text{N-AcTyr}}}{[\text{H}^+] + K_{a1}^{\text{N-AcTyr}}} \quad (6b)
\end{aligned}$$

In strongly acidic solutions, Tyr and *N*-AcTyr quench the triplet-excited TCBP with $k_{q1} = 2.1 \times 10^9$ and $k_{q1} = 2.7 \times 10^9$ $\text{M}^{-1} \text{s}^{-1}$, respectively, which is close to the diffusion-controlled limit. The quenching rate is observed to decrease with deprotonation of dye triplets at $2 < \text{pH} < 6.0$ for Tyr and *N*-AcTyr. This diminution is more pronounced for *N*-AcTyr due to the difference in the molecular net charge of the reactants $\text{TCBP}^{4-}/\text{N-AcTyrOH}$ and $\text{TCBP}^{4-}/\text{NH}_3^+\text{TyrOH}$ (like in the case of tryptophan). The quenching rate constant decreases with deprotonation of the Tyr amino group; i.e., in the pair $\text{TCBP}^{4-}/\text{NH}_2\text{TyrOH}$, k_{q4} is $(4.0\text{--}10.0) \times 10^8$ $\text{M}^{-1} \text{s}^{-1}$ (it was

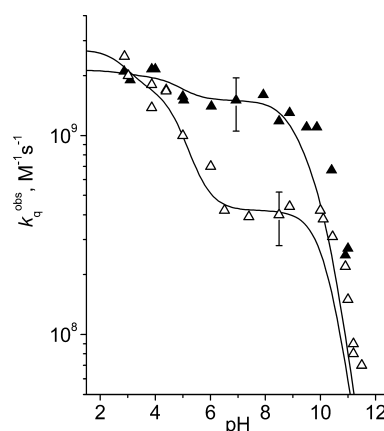


Figure 3. pH dependences of the observed quenching rate constant for the reaction of triplet TCBP with Tyr (solid triangles) and with *N*-AcTyr (open triangles). Solid lines are the simulations from eqs 6a and 6b.

impossible to determine this value to high accuracy). The quenching rate constant of *N*-AcTyr in the pH range from 6 to 10.1 does not vary with pH. Simulating the pH dependences of Tyr and *N*-AcTyr with $k_{q5} < 1.0 \times 10^6$ $\text{M}^{-1} \text{s}^{-1}$ implies that no quenching reaction occurs between the triplet TCBP^{4-} and either NH_2TyrO^- or N-AcTyrO^- . This assumption was confirmed by CIDNP measurements (see below).

CIDNP Measurements. Information about the quenching rate constants is important in both interpreting the details of CIDNP formation mechanism and optimizing the conditions for TR-CIDNP experiment. The concentrations of quenchers were adjusted to reveal the difference in reactivity between a free amino acid and its acetylated derivative. The CIDNP spectra observed under irradiation of TCBP/quencher solutions are shown in Figure 4. The polarization pattern is pH independent, except for the pH-induced changes in the chemical shifts of NMR signals. The polarization patterns for

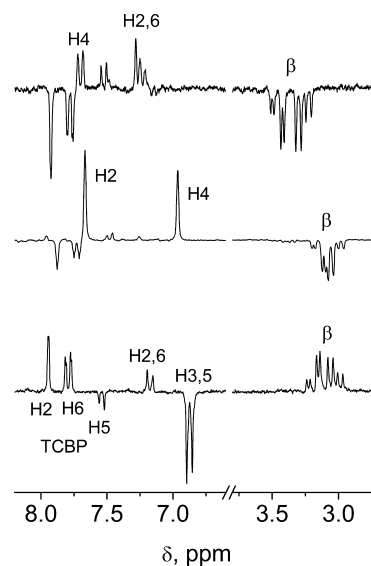


Figure 4. 200 MHz ^1H CIDNP spectra, obtained in the photoreaction of 2 mM TCBP with (top) 1.1 mM Trp in D_2O ($\text{pH}^* 7.0$), (middle) 40 mM His in D_2O at $\text{pH}^* 7.6$, and (bottom) 2.2 mM Tyr in D_2O at $\text{pH}^* 6.7$. All spectra were recorded immediately after the laser pulse with a detecting RF pulse of 1 μs .

N-acetylated derivatives are similar to those for free amino acids. The CIDNP signals are observed for the nonexchangeable protons with nonzero hyperfine couplings in the transient radicals. Pursuant to simple rules for CIDNP,³² the spin-selective radical recombination results in both the positive polarization (enhanced absorption) for the H2, H6, and H4 protons of Trp/N-AcTrp, for the H2 and H4 protons of His/N-AcHis, and for the H2,6 and β protons of Tyr/N-AcTyr and the negative polarization (emission) for the β protons of Trp/N-AcTrp, β protons of His/N-AcHis and H3,5 of Tyr/N-AcTyr. The polarization of TCBP formed in the radical pairs with tryptophanyl and histidyl radicals with $\Delta g > 0$ is positive for H5 proton and negative for H2 and H6 protons. For the pair with a tyrosyl radical with $\Delta g < 0$ the polarization of H2 and H6 protons of TCBP is positive and negative for H5 proton of TCBP.

The pH* dependences of geminate CIDNP signals are presented in Figure 5 for Trp and N-AcTrp, in Figure 6 for His,

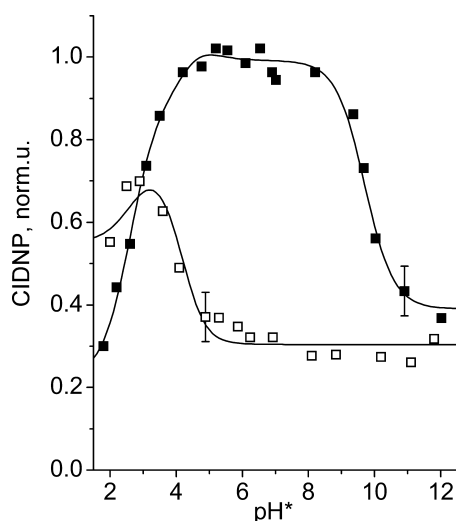


Figure 5. pH* dependences of geminate CIDNP intensity for Trp (solid squares) and N-AcTrp (open squares). Solid lines: simulations from eq 8.

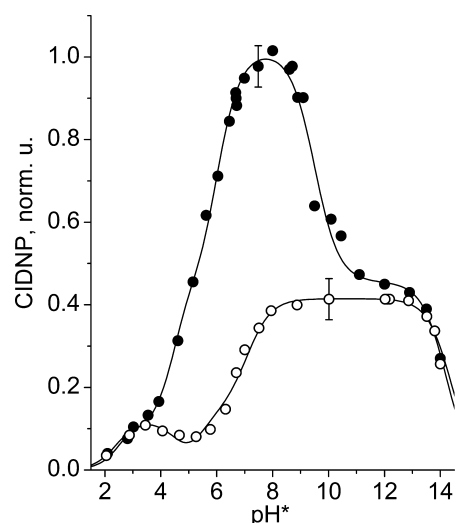


Figure 6. pH* dependences of geminate CIDNP intensity for His (solid circles) and N-AcHis (open circles). Solid lines: simulations from eq 8.

N-AcHis, and in Figure 7 for Tyr, N-AcTyr. The vertical scaling factors were chosen so that the maximum CIDNP value of

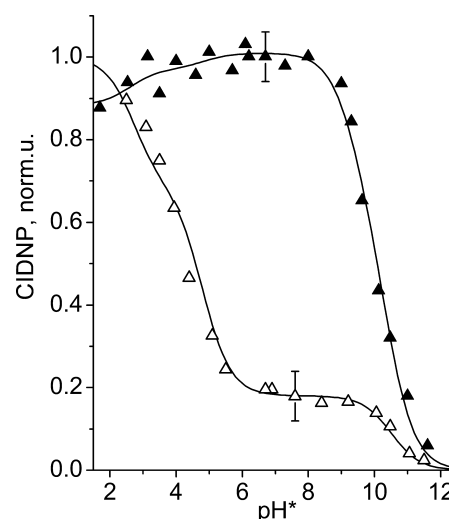


Figure 7. pH* dependences of geminate CIDNP intensity for Tyr (solid triangles) and N-AcTyr (open triangles). Solid lines: simulations from eq 8.

amino acid (Trp, His, Tyr) in each calculated curve was equal to unity, and the relative CIDNP intensities of N-acetylated derivatives were scaling correspondingly. The CIDNP pH* dependences were characterized as in the case of k_q^{obs} by dividing the pH* curve into several pH* regions with the main reactant pairs in each pH* area (Tables 1 and 2).

In general, the two factors can influence the magnitude of geminate CIDNP: the concentration of radicals (in other words, the efficiency of dye quenching) and the magnetic interactions in the radical pair. The quenching factor, q_i , characterizes the quenching efficiency and is described by the Stern–Volmer equation:

$$q_i = \frac{\alpha(\text{quencher})}{\frac{1}{k_q \tau c_0} + \alpha(\text{quencher})} \quad (7)$$

where c_0 is the quencher concentration, $\alpha(\text{quencher})$ is a molar fraction of the quencher, and τ is the intrinsic lifetime of dye triplets. In addition to the quenching rate constant k_q , each pair of reactants is characterized by polarization generated per this pair p_i (enhancement factor). If the concentration of the quencher is high enough, the quenching factor, q_i , has no effect on the geminate CIDNP intensity. The observed magnitudes of geminate polarization obey the equation:

$$I = \sum_i p_i \times q_i \times \alpha(\text{quencher}) \times \alpha(\text{dye}) \quad (8)$$

where q_i is the quenching factor, p_i is the enhancement factor, $\alpha(\text{quencher})$ and $\alpha(\text{dye})$ are the molar fractions of the quencher and the dye, respectively. The products $q_i \times p_i$ were the fitting parameters. The best-fit values of $q_i \times p_i$ are listed in Table 2.

In acidic solutions, the tryptophanyl radical exists in the protonated form $\text{TrpH}^{+\bullet}$ ($\text{pK}_a = 4.3^{29,31}$) and participates in degenerate electron exchange with the ground-state molecules, $\text{TrpH}^{+\bullet} + \text{TrpH} \xrightarrow{k_{\text{ex}}} \text{TrpH} + \text{TrpH}^{+\bullet}$. This reaction leads to polarization transfer (designated by “P”) from radical cations to

diamagnetic molecules and determines the decay of the geminate CIDNP signals of Trp and *N*-AcTrp protons at acidic pH* (Figure 5). In solutions at higher pH*, the cation radical TrpH^{•+} rapidly deprotonates to give rise to a neutral radical Trp[•]. The neutral tryptophanyl radical Trp[•] is not involved in the degenerate electron exchange reaction. In neutral and basic solutions, the CIDNP pH* dependence curves coincide with the LFP data; i.e., a decrease of geminate polarization is observed due to the deprotonation of the Trp amino group, whereas the geminate CIDNP of *N*-AcTrp is pH* independent in the pH* range from 5.5 to 12.

The inflection points of the CIDNP titration curves for His and *N*-AcHis (Figure 6) correlate both with the p*K*_a values of the protonation states of amino acids and the dye and with the *k*_q^{obs} dependences. In strongly acidic solutions (pH* < 2), TCBP and amino acids (His or *N*-AcHis) are protonated, and no geminate polarization is observed. At 2 < pH* < 7.2 (for His) and 2 < pH* < 8.2 (for *N*-AcHis) the geminate polarization increases with deprotonation of dye triplets and amino acids (imidazolyl of His or *N*-AcHis becomes neutral). Upon deprotonation of the terminal histidine amino group, the geminate CIDNP signals decrease by more than a factor of 2 (pH* ranging from 7.1 to 12). The geminate CIDNP intensity of *N*-acetylhistidine does not change with pH* varying from 8.2 to 12.

Though we failed to measure the quenching rate constant at pH > 12 for the reactant pairs TCBP⁴⁻/NH₂His⁻ and TCBP⁴⁻/*N*-AcHis⁻, we obtained the dependence of CIDNP on pH* for His and *N*-AcHis at pH* > 12. In highly basic solutions imidazolyl of histidine and its *N*-acetyl derivative releases the last proton. This process is accompanied by a high field shift of H2, H4 protons in NMR spectrum and a decrease of CIDNP signals of His and *N*-AcHis. The best-fit simulations yielded acidity constants for the last titratable proton: 14.2 for His and 14.4 for *N*-AcHis. The drop of CIDNP at pH* > 12 means that the quenching rate constant of TCBP triplets by His or *N*-AcHis with negatively charged imidazolyl is much lower than in the case of these amino acids with neutral imidazolyl. This observation is in correlation with the drop of the quenching rate constant of TCBP triplets by Tyr or *N*-AcTyr upon the release of the phenolic proton.

The CIDNP titration curves for Tyr and *N*-AcTyr (Figure 7) are determined by the same p*K*_a values as the *k*_q^{obs} pH dependences. The maximum CIDNP intensity is observed in acidic and neutral solutions. The deprotonation of the Tyr amino group decreases the geminate CIDNP intensity. For the reactant pairs TCBP⁴⁻/NH₂TyrO⁻ and TCBP⁴⁻/*N*-AcTyrO⁻, no geminate polarization was observed.

DISCUSSION

As shown earlier, the quenching rate constants of the reaction between the photoexcited triplet dyes and amino acids, close to the diffusion controlled limit (*k* ≥ 10⁹ M⁻¹ s⁻¹), are typical of electron transfer reactions.^{22,33} Therefore, the electron transfer is assumed to be the mechanism of triplet TCBP quenching by Trp, *N*-AcTrp, Tyr, and *N*-AcTyr in acidic solution, at both pH < 2.9 and 2.9 < pH < 4.9. As follows from Table 2, the deprotonation of ³TCBPH₄ to ³TCBPH₂²⁻ results in no noticeable change in *k*_q^{obs} for Trp (3.5 × 10⁹ M⁻¹ s⁻¹) and a slight decrease in *k*_q^{obs} from 2.1 × 10⁹ to 1.9 × 10⁹ for Tyr. The quenching rate constant of the triplet TCBP, *k*_q^{obs}, is observed to decrease with increasing pH upon deprotonation of ³TCBPH₄ in the case of *N*-acetyl derivatives of amino acids,

from the value 3.4 × 10⁹ to 2.1 × 10⁹ M⁻¹ s⁻¹ for *N*-AcTrp, and from the value 2.7 × 10⁹ to 1.7 × 10⁹ M⁻¹ s⁻¹ for *N*-AcTyr. This decrease in chemical reactivity between the triplet TCBP and *N*-AcTyr or *N*-AcTrp in the TCBPH₄ > TCBPH₂²⁻ order can be explained by Coulombic interaction (repulsion) between the negatively charged reactants at 2.9 < pH < 4.9 as compared to neutral reactants at pH < 2.9. In the case of either Trp or Tyr, one of the reactants in the pair carries no net charge in both pH regions, pH < 2.9 and 2.9 < pH < 4.9, which results in the equal or nearly equal values of quenching rate constants.

Let us consider the mechanism of ³TCBP⁴⁻ quenching. When electron transfer is the only possible reaction mechanism, which holds for both Tyr and *N*-AcTyr at pH > 10.1, and His and *N*-AcHis at pH > 14.3, no reaction is detected. This indicates that the proton is involved in the quenching reaction, which becomes undetectable in the absence of transferable proton at the reactive residue. An alternative explanation is that the Coulombic repulsion between reactants could also slow down the quenching reaction at pH values higher than p*K*_a both of the phenolic proton of Tyr and *N*-AcTyr, and of the last titratable proton of His and *N*-AcHis. However, such a dramatic effect of Coulombic interaction, which makes the quenching reaction undetectable, is unlikely.

For all studied amino acids with no charge at the amino group and with transferrable proton at the reaction center available, the quenching rate constants are of the same order of magnitude and coincide for acetylated and nonacetylated amino acids (8.0 × 10⁸ M⁻¹ s⁻¹ for Trp and 7.8 × 10⁸ M⁻¹ s⁻¹ for *N*-AcTrp; 3.0 × 10⁸ M⁻¹ s⁻¹ for His and 3.1 × 10⁸ M⁻¹ s⁻¹ for *N*-AcHis; 4.2 × 10⁸ M⁻¹ s⁻¹ for *N*-AcTyr; (4–10) × 10⁸ M⁻¹ s⁻¹ for Tyr, which could not be determined with fair accuracy). This indirectly confirms a crucial role of labile proton at the reaction center in the formation of radicals by TCBP⁴⁻ quenching. Using only our methods, we cannot discriminate a sequence of individual steps of electron and proton transfer in reactions and cannot even say which of the quenching process mechanisms (sequential or concert) is operative.

For nonacetylated amino acids, there is an additional pair of reactants that includes amino acid with a positively charged amino group. The quenching rate constants are 2.2 × 10⁹ M⁻¹ s⁻¹ for Trp, 1.5 × 10⁹ M⁻¹ s⁻¹ for Tyr, and 1.6 × 10⁹ M⁻¹ s⁻¹ for His, which is 3–5 times as high as the corresponding values for amino acids with the uncharged amino group. In our opinion, this could be attributed to the absence of Coulombic repulsion in the reactants' pair due to the zero net charge of amino acid with the positively charged amino group and with the negatively charged carboxylic group (Table 2). On the other hand, these quenching rate constants are lower than those of ³TCBPH₂²⁻ quenching by tryptophan and tyrosine, where the most probable reaction mechanism is electron transfer. It is assumed then that the mechanism of ³TCBP⁴⁻ quenching by amino acids is the proton coupled electron transfer, which is slowed down when the Coulombic repulsion between the reactants takes place.

The influence of Coulombic interaction is also confirmed by CIDNP measurements. The signal amplitude of geminate CIDNP for nonacetylated amino acids with a positively charged amino group was always much higher than that for either the corresponding *N*-acetylated derivatives or amino acids with a neutral amino group. This was assigned to the influence of electrostatic repulsion, which significantly decreases the lifetime

of transient radical pairs as compared to the case where electrostatic interaction is absent.

To clarify the influence of amino group on the reactivity of amino acids toward the triplet-excited TCBP, we have obtained the pH^* dependences of the geminate CIDNP for dipeptides in which only one residue is reactive toward $^3\text{TCBP}$, namely, for His-Phe and Phe-His, and also for His-His. Figure 8 shows the

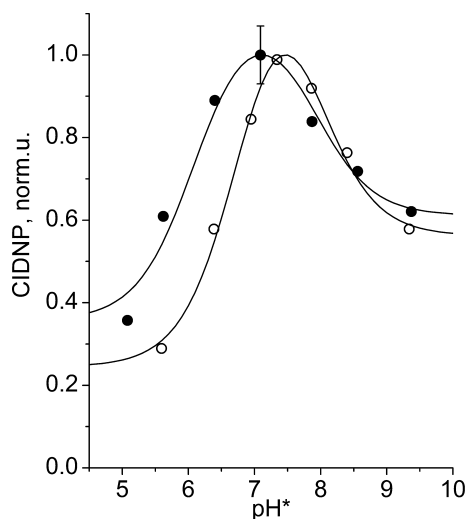


Figure 8. pH^* dependences of geminate CIDNP intensity for His-Phe (solid circles) and Phe-His (open circles). Solid lines: simulations from eq 8.

pH^* dependences of geminate CIDNP obtained in the photoreaction of TCBP with His-Phe and Phe-His at different pH^* . For both dipeptides, the polarization of only the His moiety is observed (the corresponding CIDNP spectra are given in the Supporting Information). This indicates that, as expected, the phenylalanine residue is not involved in the quenching reaction. The CIDNP titration curves are similar to the pH^* dependence of geminate CIDNP for His at neutral and basic pH^* . The increase in geminate polarization is caused by deprotonation of the positively charged imidazolyl of Phe-His ($\text{pK}_a^* = 6.8$) and His-Phe ($\text{pK}_a^* = 6.1$). The deprotonation of the amino group of both dipeptides ($\text{pK}_a^* = 7.9$) decreases the geminate CIDNP signals by a factor of 1.7. Thus, the reactivity of these dipeptides depends on the protonation state of both imidazolyl and amino group disregarding the location of the histidyl residue.

The same tendency was observed under irradiation of the TCBP and His-His dipeptide solutions at different pH^* . In this case, both of the residues are involved in the quenching of the triplet-excited TCBP, resulting in the formation of the dipeptide radicals of two types, with radical centers on either the C- or the N-terminal His-His residues (corresponding CIDNP spectra are shown in the Supporting Information). For pH^* above 5.5, a growth of geminate CIDNP for both residues is observed in accordance with the acidity constants of imidazolyl moieties at N- and C-terminus, $\text{pK}_{\text{a1-N}}^* = 5.7$, $\text{pK}_{\text{a2-C}}^* = 6.8$, respectively. When pH^* is above $\text{pK}_{\text{a2-C}}^* = 6.8$, the CIDNP signals of the N- and C-terminal residues become nearly equal, pointing to a very close reactivity of two residues. With the pH^* exceeding the pK_a^* of the terminal amino group (8.0) CIDNP is observed to decrease for both of the residues. As in the case of the His-Phe and Phe-His dipeptides, removing

a positive charge of the His-His amino group causes a 2–3-fold decrease in the efficiency of $^3\text{TCBP}$ quenching.

Now let us consider the quenching reaction mechanism for histidine with the positively charged imidazolyl moiety. In acidic solutions, the pH dependences of k_q^{obs} for histidine differ totally from those for tryptophan and tyrosine. Under strong acidic conditions ($\text{pH} < 2.9$), no quenching of $^3\text{TCBP}$ by $\text{NH}_3^+\text{HisH}_2^+$ and $N\text{-AcHisH}_2^+$ is observed, whereas for tryptophan and tyrosine k_q^{obs} is maximal. Upon deprotonation of $^3\text{TCBP}$, k_q^{obs} for histidine first increases and then decreases, passing through a maximum for $^3\text{TCBP}^{2-}$. A distinct difference in the pH dependences of the observed quenching rate constants for tryptophan (tyrosine) and histidine gives us the clue to understanding that within this range, the mechanism of quenching by these amino acids is different. For tryptophan (tyrosine), $^3\text{TCBP}$ is quenched via electron transfer, which is impossible for histidine in strongly acidic conditions: electron removal from both $\text{NH}_3^+\text{HisH}_2^+$ and $N\text{-AcHisH}_2^+$ would lead to the formation of the highly unstable dicationic imidazolyl radical. It is concluded then that the quenching by histidine should proceed either via hydrogen atom transfer or via electron transfer accompanied by proton transfer prior or after electron removal from amino acid. We have found evidence that the concept of electron transfer preceded by proton transfer is appropriate and allows us to qualitatively explain all the peculiarities of pH dependence detected for the quenching by histidine. First, it was found that the quenching of the fully protonated $^3\text{TCBP}$ by histidine in acidic conditions either proceeds with an extremely low rate or does not take place at all. This indicates that hydrogen transfer to carbonyl group is inefficient. Moreover, this is in accordance with the PCET mechanism because there is no vacancy on the dye for proton transfer from imidazolyl moiety when all carboxylic groups of TCBP are protonated. Second, an increase in the quenching rate constant with pH can be explained by the fact that upon $^3\text{TCBP}^{2-}$ deprotonation, there appear the vacancies for proton transfer to the dye.

A decrease in k_q^{obs} upon $^3\text{TCBP}^{2-}$ deprotonation into $^3\text{TCBP}^{4-}$ can be assigned to the fact that the quenching of $^3\text{TCBP}^{4-}$ proceeds via PCET, as established for tyrosine, tryptophan, and histidine with the uncharged imidazolyl moiety, and additional proton transfer from histidine is needed. Thus, the quenching reaction requires the transfer of one electron and two protons, resulting in a 4 times decrease of the quenching rate constant for both His and $N\text{-AcHis}$ when the protonation state of the dye changes from $^3\text{TCBP}^{2-}$ to $^3\text{TCBP}^{4-}$: $4.3 \times 10^8 \text{ M}^{-1} \text{ s}^{-1}$ versus $1.0 \times 10^8 \text{ M}^{-1} \text{ s}^{-1}$ for His, and $7.7 \times 10^7 \text{ M}^{-1} \text{ s}^{-1}$ versus $1.9 \times 10^7 \text{ M}^{-1} \text{ s}^{-1}$ for $N\text{-AcHis}$. The corresponding values for His are 5 times as high as that for $N\text{-AcHis}$, which is attributed to electrostatic attraction of reactants in the case of His. It is worth noting that the lower the reactivity is, the higher is the influence of the Coulombic interaction on the quenching rate constant observed.

The deprotonation of the imidazolyl moiety of histidine switches the reaction mechanism to PCET, and the reactivity of histidine becomes comparable to that of tyrosine and tryptophan, as discussed above.

CONCLUSIONS

In the present work, a study is made of the photochemical reaction between 3,3',4,4'-benzophenonetetracarboxylic acid (TCBP) and aromatic amino acids, His, Trp, and Tyr. We have

compared the reactivities of free His, Trp, and Tyr and their acetylated derivatives, *N*-AcHis, *N*-AcTyr, and *N*-AcTrp toward the TCBP triplets in the pH range 2–12 of aqueous solution to establish the reaction mechanism and the effect of reactant net charge on the oxidation of the highly reactive amino acid moieties. A complementary application of laser flash photolysis and time-resolved CIDNP enabled us to monitor transient triplet intermediates and to get information on transient radical intermediates at the geminate stage of the reaction. As a result, the pH dependences of CIDNP amplitudes and the rate constants of the quenching of TCBP triplets by His, Tyr, and Trp, as well as *N*-AcHis, *N*-AcTyr, and *N*-AcTrp were revealed and explained in terms of pK_a 's of reactants and reaction mechanisms.

The following conclusions can be drawn from our data on the reaction mechanism of triplet TCBP quenching by amino acids.

Combining the data on the pH dependences of both the geminate CIDNP and the quenching rate for histidine and tyrosine, we have established that the proton transfer to free radical formation is involved in the quenching reaction of electron transfer. Thus, PCET is the mechanism of the quenching of the fully deprotonated dye, $^3\text{TCBP}^{4-}$, by all amino acids whereas $^3\text{TCBP}^{2-}$ and $^3\text{TCBP}^{4-}$ react with tyrosine and tryptophan via electron transfer. Histidine with positively charged imidazolyl is less reactive than histidine with neutral imidazolyl, because the reaction of the former requires additional proton transfer.

The Coulombic interaction was found to influence the observed quenching rate constants. This effect is more pronounced in the case of the lower reactivity of participating species. The signal amplitude of geminate CIDNP has also appeared to depend on electrostatic interaction which changes the lifetime of transient radical pairs despite the high polarity of the solvent.

Usually, the reactivity of histidine toward the triplet-excited dyes is much lower than that of tryptophan and tyrosine.^{13–17} To the best of our knowledge, TCBP is the only dye, the excited triplets of which could be quenched with comparable efficiencies by tryptophan, tyrosine, and histidine in neutral to basic aqueous solutions. This makes it possible to study the reaction of electron transfer from tyrosine and tryptophan to histidyl radical by TR-CIDNP. Though the reaction of intramolecular electron transfer from tyrosine to histidyl radical in oxidized peptides His-Tyr and Tyr-His was detected by means of TR-CIDNP, the use of 2,2'-dipyridyl as a photosensitizer, has limited our observations to a single pH value, at which the histidyl radical could be generated in concentration high enough to produce detectable CIDNP intensity.¹² TCBP seems to be a promising photosensitizer in studying the reactions involving histidyl radical.

■ ASSOCIATED CONTENT

■ Supporting Information

125 MHz ^{13}C NMR of 3,3',4,4'-benzophenonetetracarboxylic acid. 200 MHz ^1H spectra of 3,3',4,4'-benzophenonetetracarboxylic acid, *L*-phenylalanine-*L*-histidine, *L*-histidine-*L*-phenylalanine, and *L*-histidine-*L*-histidine. Chemical shift titration curves of 3,3',4,4'-benzophenonetetracarboxylic acid, *L*-histidine-*L*-phenylalanine, *L*-phenylalanine-*L*-histidine, and *L*-histidine-*L*-histidine. 200 MHz ^1H CIDNP spectra of *L*-histidine-*L*-phenylalanine, *L*-phenylalanine-*L*-histidine, and *L*-histidine-*L*-

histidine. This information is available free of charge via the Internet at <http://pubs.acs.org>.

■ AUTHOR INFORMATION

Corresponding Author

*A. V. Yurkovskaya: tel, +7 383 3331333; fax, +7 383 3331399; e-mail, yurk@tomo.nsc.ru.

Notes

The authors declare no competing financial interest.

■ ACKNOWLEDGMENTS

We are grateful to Prof. Dr. Vladimir N. Silnikov and Ms. Lubov A. Yarinich for the synthesis of *L*-phenylalanine-*L*-histidine dipeptide. This work was supported by the program of the Russian Government "Measures to Attract Leading Scientists to Russian Educational Institutions" (Grant No. 11.G34.31.0045), RFBR (Project Nos. 13-03-00437, 12-03-33082, 14-03-00453), Program of the Division of Chemistry and Material Science RAS (Project 5.1.1), and Grant No. MD-3279.2014.2 of the President of the Russian Federation". Natalya N. Saprygina thanks the Austrian Academic Exchange Service (ÖAD) for the scholarships at Graz University of Technology within the Eurasia-Uninet Network Program and EU FP7 COST Program TD1103 "European Network for Hyperpolarization Physics and Methodology in NMR and MRI".

■ REFERENCES

- (1) Stuart-Audette, M.; Blouquit, Y.; Faraggi, M.; Sicard-Roselli, C.; Houee-Levin, C.; Jolles, P. Re-Evaluation of Intramolecular Long-Range Electron Transfer Between Tyrosine and Tryptophan in Lysozymes. Evidence for the Participation of Other Residues. *Eur. J. Biochem.* **2003**, *270*, 3565–3571.
- (2) Gao, J.; Muller, P.; Wang, M.; Eckhardt, S.; Lauz, M.; Fromm, K. M.; Giese, B. Electron Transfer in Peptides: the Influence of Charged Amino Acids. *Angew. Chem., Int. Ed.* **2011**, *50*, 1926–1930.
- (3) Cordes, M.; Giese, B. Electron Transfer in Peptides and Proteins. *Chem. Soc. Rev.* **2009**, *38*, 892–901.
- (4) Lauz, M.; Eckhardt, S.; Fromm, K. M.; Giese, B. The Influence of Dipole Moments on the Mechanism of Electron Transfer through Helical Peptides. *Phys. Chem. Chem. Phys.* **2012**, *14*, 13785–13788.
- (5) Sibert, R.; Josowicz, M.; Porcelli, F.; Veglia, G.; Range, K.; Barry, B. A. Proton-Coupled Electron Transfer in a Biomimetic Peptide as a Model of Enzyme Regulatory Mechanisms. *J. Am. Chem. Soc.* **2007**, *129*, 4393–4400.
- (6) Biskup, T.; Paulus, B.; Okafuji, A.; Hitomi, K.; Getzoff, E. D.; Weber, S.; Schleicher, E. Variable Electron Transfer Pathways in an Amphibian Cryptochrome: Tryptophan Versus Tyrosine-Based Radical Pairs. *J. Biol. Chem.* **2013**, *288*, 9249–9260.
- (7) Prütz, W. A.; Butler, J.; Land, E. J.; Swallow, A. J. Direct Demonstration of Electron-Transfer between Tryptophan and Tyrosine in Proteins. *Biochem. Biophys. Res. Commun.* **1980**, *96*, 408–414.
- (8) Faraggi, M.; DeFelippis, M. R.; Klapper, M. H. Long-Range Electron Transfer Between Tyrosine and Tryptophan in Peptides. *J. Am. Chem. Soc.* **1989**, *111*, 5141–5145.
- (9) Reece, S. Y.; Seyedsayamdost, M. R.; Stubbe, J.; Nocera, D. G. Photoactive Peptides for Light-Initiated Tyrosyl Radical Generation and Transport into Ribonucleotide Reductase. *J. Am. Chem. Soc.* **2007**, *129*, 8500–8509.
- (10) Morozova, O. B.; Kaptein, R.; Yurkovskaya, A. V. Changing the Direction of Intramolecular Electron Transfer in Oxidized Dipeptides Containing Tryptophan and Tyrosine. *J. Phys. Chem. B* **2012**, *116*, 12221–12226.
- (11) Morozova, O. B.; Yurkovskaya, A. V.; Sagdeev, R. Z. Reversibility of Electron Transfer in Tryptophan-Tyrosine Peptide in

Acidic Aqueous Solution Studied by Time-Resolved CIDNP. *J. Phys. Chem. B* **2005**, *109*, 3668–3675.

(12) Morozova, O. B.; Yurkovskaya, A. V. Intramolecular Electron Transfer in the Photooxidized Peptides Tyrosine–Histidine and Histidine–Tyrosine: A Time-Resolved CIDNP Study. *Angew. Chem., Int. Ed.* **2010**, *49*, 7996–7999.

(13) Muszkat, K. A.; Wismontski-Knittel, T. Reactivities of Tyrosine, Histidine, Tryptophan, and Methionine in Radical Pair Formation in Flavin Triplet Induced Protein Nuclear Magnetic Polarization. *Biochemistry* **1985**, *24*, 5416–5421.

(14) Huvaere, K.; Skibsted, L. H. Light-Induced Oxidation of Tryptophan and Histidine. Reactivity of Aromatic N-Heterocycles Toward Triplet-Excited Flavins. *J. Am. Chem. Soc.* **2009**, *131*, 8049–8060.

(15) Heelis, P. F.; Parsons, B. J.; Phillips, G. O. The pH Dependence of the Reactions of Flavin Triplet States with Amino Acids. A Laser Flash Photolysis Study. *Biochim. Biophys. Acta* **1979**, *587*, 455–462.

(16) Morozova, O. B.; Yurkovskaya, A. V.; Tsentalovich, Y. P.; Forbes, M. D. E.; Hore, P. J.; Sagdeev, R. Z. Time Resolved CIDNP Study of Electron Transfer Reactions in Proteins and Model Compounds. *Mol. Phys.* **2002**, *100*, 1187–1195.

(17) Tsentalovich, Y. P.; Lopez, J. J.; Hore, P. J.; Sagdeev, R. Z. Mechanisms of Reactions of Flavin Mononucleotide Triplet With Aromatic Amino Acids. *Spectrochim. Acta, Part A* **2002**, *58A*, 2043–2050.

(18) Battacharyya, S. N.; Das, P. K. Photoreduction of Benzophenone by Amino-Acids, Aminopolycarboxylic Acids and Their Metal-Complexes - a Laser-Flash-Photolysis Study. *J. Chem. Soc., Faraday Trans.* **1984**, *80*, 1107–1116.

(19) Morozova, O. B.; Kiryutin, A. S.; Sagdeev, R. Z.; Yurkovskaya, A. V. Electron Transfer between Guanosine Radical and Amino Acids in Aqueous Solution. I. Reduction of Guanosine Radical by Tyrosine. *J. Phys. Chem. B* **2007**, *111*, 7439–7448.

(20) Krezel, A.; Bal, W. A Formula for Correlating pKa Values Determined in D₂O and H₂O. *J. Inorg. Biochem.* **2004**, *98*, 161–166.

(21) Nelson, D. L.; Michael, C. M. *Lehninger Principles of Biochemistry*, 3rd ed.; Worth Publishers: New York, 2000.

(22) Tsentalovich, Y. P.; Morozova, O. B.; Yurkovskaya, A. V.; Hore, P. J.; Sagdeev, R. Z. Time-Resolved CIDNP and Laser Flash Photolysis Study of the Photoreactions of N-Acetylhistidine with 2,2'-Dipyridyl in Aqueous Solution. *J. Phys. Chem. A* **2000**, *104*, 6912–6916.

(23) Weber, O. A. Stability of Proton and Cu(II) Complexes of Some Tyrosine and Tryptophan Derivatives. *J. Inorg. Nucl. Chem.* **1974**, *36*, 1341–1347.

(24) Saprygina, N. N.; Morozova, O. B.; Gritsan, N. P.; Fedorova, O. S.; Yurkovskaya, A. V. ¹H CIDNP Study of the Kinetics and Mechanism of the Reversible Photoinduced Oxidation of Tryptophyl-Tryptophan Dipeptide in Aqueous Solutions. *Russ. Chem. Bull.* **2011**, *60*, 2579–2587.

(25) Nguyen, T. X.; Kattnig, D.; Mansha, A.; Grampp, G.; Yurkovskaya, A. V.; Lukzen, N. Kinetics of Photoinduced Electron Transfer between DNA Bases and Triplet 3,3',4,4'-Benzophenone Tetracarboxylic Acid in Aqueous Solution of Different pH's: Proton-Coupled Electron Transfer? *J. Phys. Chem. A* **2012**, *116*, 10668–10675.

(26) Inbar, S.; Linschitz, H.; Cohen, S. G. Nanosecond Flash Studies of Reduction of Benzophenone by Aliphatic Amines. Quantum Yields and Kinetic Isotope Effects. *J. Am. Chem. Soc.* **1981**, *103*, 1048–1054.

(27) Bansal, K. M.; Fessenden, R. W. Pulse Radiolysis Studies of the Oxidation of Phenols by SO₄^{•−} and Br^{2•} in Aqueous Solutions. *Radiat. Res.* **1976**, *67*, 1–8.

(28) Santus, R.; Bazin, M.; Aubailly, M.; Guernonprez, R. Influence of Energy Transfer on the Photoionization of Tryptophan and Tyrosine in Basic Media. *Photochem. Photobiol.* **1972**, *15*, 61–69.

(29) Baugher, J. F.; Grossweiner, L. I. Photolysis Mechanism of Aqueous Tryptophan. *J. Phys. Chem.* **1977**, *81*, 1349–1354.

(30) Yurkovskaya, A. V.; Snytnikova, O. A.; Morozova, O. B.; Tsentalovich, Y. P.; Sagdeev, R. Z. Time-Resolved CIDNP and Laser Flash Photolysis Study of the Photoreaction between Triplet 2,2'-

Dipyridyl and Guanosine-5'-Monophosphate in Water. *Phys. Chem. Chem. Phys.* **2003**, *5*, 3653–3659.

(31) Evans, R. F.; Ghiron, C. A.; Volkert, W. A.; Kuntz, R. R. Flash Photolysis of N-Acetyl-L-Tryptophanamide; Acid-Base Equilibrium of the Radical Transients. *Chem. Phys. Lett.* **1976**, *42*, 43–45.

(32) Kaptein, R. Simple Rules for Chemically Induced Dynamic Nuclear Polarization. *J. Chem. Soc., Chem. Commun.* **1971**, 432, 732–733.

(33) Tsentalovich, Y. P.; Morozova, O. B.; Yurkovskaya, A. V.; Hore, P. J. Kinetics and Mechanism of the Photochemical Reaction of 2,2'-Dipyridyl with Tryptophan in Water: Time-Resolved CIDNP and Laser Flash Photolysis Study. *J. Phys. Chem. A* **1999**, *103*, 5362–5368.